Methanol Dehydrogenation and Formation of Carbonaceous Overlayers on Pd(111) Studied by High-Pressure SFG and XPS Spectroscopy

M. Morkel, V. V. Kaichev,† G. Rupprechter,* and H.-J. Freund

Fritz Haber Institute, Faradayweg 4-6, D-14195 Berlin, Germany

I. P. Prosvirin and V. I. Bukhtiyarov

Boreskov Institute of Catalysis, Lavrentieva ave. 5, Novosibirsk 630090, Russia

Received: April 28, 2004; In Final Form: June 16, 2004

Methanol decomposition on Pd(111) at 300 and 400 K was studied in situ from 5×10^{-7} to 0.1 mbar by combining vibrational sum frequency generation (SFG) and X-ray photoelectron spectroscopy (XPS). Two competing decomposition pathways, i.e., dehydrogenation of CH_3OH to CO and H_2 and methanolic C−O bond scission, were observed by monitoring the time-dependent evolution of CO/CH_xO and of carbonaceous deposits CH_x ($x = 0-3$) via their vibrational and photoemission characteristics. Quantification of carbon-containing species was performed by XPS, while the preferred binding site of CH_x was determined by SFG using CO as probe molecule for postreaction adsorption. In contrast to previous reports, Pd(111) was found to be quite active for methanolic C−O bond scission. The CH_x formation rate strongly increased with pressure and temperature, leading to immediate catalyst deactivation at 0.1 mbar and 400 K. The combined SFG/XPS data suggest that the carbonaceous residues are highly dehydrogenated, such as CH or carbon atoms bonded to hollow sites. Complete dehydrogenation of CH_x species and partial dissolution of atomic carbon in the Pd bulk most likely occurred even at 300 K. On the other hand, the CH_x species was found to be unexpectedly thermally stable (up to ∼600 K), until carbon dissolution and formation of carbon clusters take place. Regeneration with oxygen above 400 K was able to remove CH_x deposits and to partially restore the initial adsorption properties. Corresponding experiments with CO did not produce any carbon signals, indicating that the cleavage of the C−O bond must occur via CH_xO intermediates (and not within CO). Methanol decomposition at pressures up to 15 mbar and temperatures up to 550 K, followed by gas chromatography, did not produce measurable decomposition products, due to fast carbon poisoning under catalytic reaction conditions.

Introduction

The decomposition (dehydrogenation) of methanol to carbon monoxide and hydrogen on supported catalysts has attracted much attention, resulting from its practical relevance to methanol-fueled vehicles or heat-recovery techniques (e.g. refs 1−4 and references therein). Although CH_3OH decomposition occurs on Pd-based catalysts with high selectivity toward CO/H_2 (rather than to CH_4 and H_2O), the overall activity is not satisfactory and is limited by catalyst deactivation.[4] The main reason for deactivation is the formation of carbon or carbonaceous species (CH_x; $x = 0-3$) by cleavage of the methanolic C−O bond (i.e. the C−O bond within a CH_xO molecule; $x = 1-4$). The dissociation of the reaction product CO is less likely but can also not be fully excluded as the source of carbon.[5−8] In this respect, methanol decomposition on Pd(111) may serve as a simple model system that allows one to study the different bond scission routes (O−H, C−H, and C−O) governing selectivity and also deactivation by carbonaceous species.

In a similar way, C−O bond scission and C−H and O−H bond formation determine the selectivity of CO hydrogenation on supported Pd catalysts (CH_3OH vs CH_4 as main products),[9−11] and Pd(111) may again serve as model catalyst. However, since CO hydrogenation does not proceed at the low pressures of ultrahigh vacuum (UHV), many studies dealt with the reverse reaction, i.e., CH_3OH decomposition.[12−31] According to the microscopic reversibility principle, CH_3OH dehydrogenation and CH_3OH synthesis should pass through the same intermediate steps.

Despite numerous reports, the exact mechanism of methanol decomposition is still under debate, because the reported results are sometimes rather controversial. Although there is agreement that the dehydrogenation of methanol to CO and H_2 occurs via methoxy (CH_3O) as first intermediate and is followed by stepwise hydrogen abstraction to CH_2O, CHO, and CO,[12−22,31] the exact mechanism and probability of *methanolic C−O bond scission* is still under discussion. Moreover, a number of UHV studies did not report any C−O bond scission at all.[13,18−21]

To explain these discrepancies, previous reports suggested that methanolic C−O bond scission on Pd(111) may proceed on surface defects[14,17,25−27] or require near-monolayer methanol coverages.[23,24,32] The first suggestion was recently supported by studies reporting that methanolic C−O bond scission preferentially takes place at or near the edges of Pd nanoparticles.[28,33] Another reason for the contrasting reports may be simply related to the kinetics of the different routes of methanol

* Corresponding author. Tel: +49 30 8413 4132. Fax: +49 30 8413 4105. E-mail: rupprechter@fhi-berlin.mpg.de.

† Permanent address: Boreskov Institute of Catalysis, Novosibirsk, Russia.

10.1021/jp048149a CCC: $27.50
Published on Web 07/31/2004

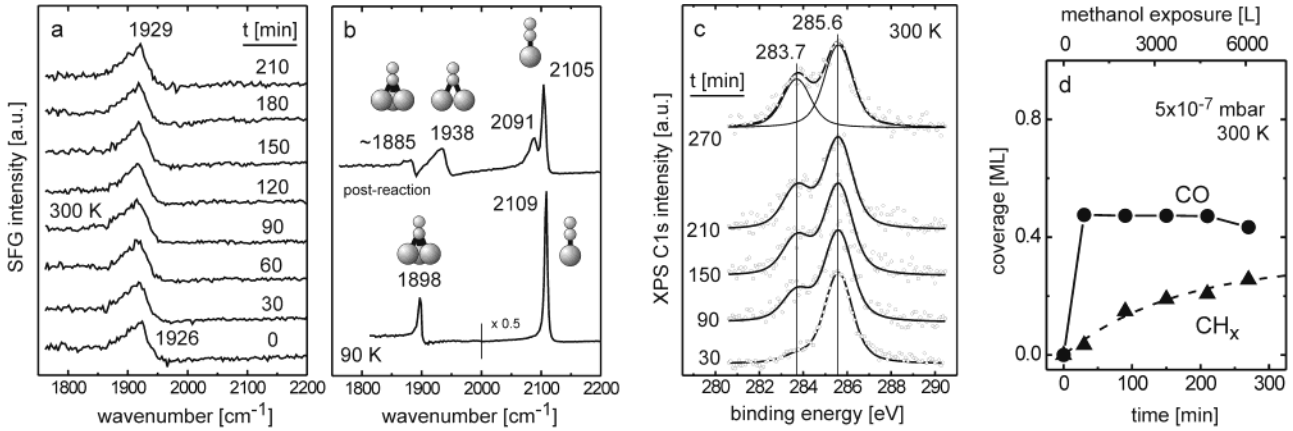

Figure 1. SFG (a) and XPS C1s core-level (c) spectra measured during exposure of Pd(111) to 5×10^{-7} mbar of methanol at 300 K. The quantitative analysis of the XPS spectra is shown in panel d, and pre- and postreaction CO adsorption is compared in panel b. The dashed line in d is the calculated rate of CH_x formation obtained by assuming a simple kinetic model in which the CH_x formation rate is proportional to the number of vacant sites; see the text.

decomposition. Beside the fast dehydrogenation, methanolic C−O bond scission most likely *also* takes place on a smooth palladium surface, but at a low rate that is difficult to measure in typical UHV experiments. Consequently, high methanol pressures, similar to those of catalytic reactions, are presumably necessary to produce noticeable amounts of carbon species through methanolic C−O bond scission.

To better understand the mechanism of methanol decomposition and to examine the ideas discussed above, we have studied the interaction of CH_3OH with smooth Pd(111) from 5×10^{-7} to 15 mbar at 300−550 K. Our approach combines vibrational sum-frequency generation (SFG) and X-ray photoelectron spectroscopy (XPS). Both methods can be applied from UHV up to mbar pressures, still providing surface-sensitive information, and are thus well-suited to monitor methanol decomposition in situ. As suggested above, at elevated pressure a considerable amount of methanolic C−O bond scission was observed even on Pd(111). The origin, nature, and stability of CH_x species were also addressed. Recently, we have utilized the same approach to study CO adsorption on well-annealed and "defect-enriched" Pd(111) from UHV up to mbar pressures.[8] No indications for CO dissociation were found. For a detailed description of the CO/Pd(111) adsorption system we refer to refs 34 and 35 and references therein.

Experimental Section

SFG spectroscopy was performed in a UHV surface analysis system combined with an SFG-compatible UHV−high-pressure cell as described previously.[36,37] The sample surfaces were characterized with low-energy electron diffraction (LEED), Auger electron spectroscopy (AES), and temperature-programmed desorption (TPD). For details about SFG spectroscopy, we refer to the literature (e.g. refs 37−43 and references therein). The SFG spectra were fitted according to eqs 1 and 2 in ref 44 to obtain the exact values of the resonance frequency.

The XPS experiments were carried out using a VG ESCALAB high-pressure electron spectrometer. Its construction has been described elsewhere.[8,45] In short, this setup is equipped with X-ray and UV−photoelectron spectroscopy (XPS/UPS), LEED, and mass spectrometry (MS). A special gas cell incorporated in the analyzer chamber of the spectrometer allows us to measure in situ XPS and UPS spectra at pressures up to 0.5 mbar. XPS spectra were taken using the Al Kα irradiation and were calibrated against $E_b(Pd3d_{5/2}) = 334.9$ eV. Quantitative analysis was carried out by fitting the experimental data as described below, using the 0.5 ML saturation structure of CO on Pd(111) at 10^{-6} mbar/300 K as reference.[8,35]

Pd(111) (99.99%) was prepared by standard cutting and polishing techniques. The crystal was mounted between Ta or W wires and could be heated to 1300 K and cooled to 90 K. Its temperature was measured with a chromel−alumel thermocouple spot-welded to the edge of the crystal. The Pd(111) surface was cleaned by a sequence of flash annealing to 1250 K, Ar ion etching at 300 K, heating to 1200 K, oxidation during cooling in 5×10^{-7} mbar of O_2 between 1200 and 600 K, and final flash to 1200 K in UHV. After a few cycles, no contaminants were registered by XPS or AES, and the surface was characterized by a sharp (1×1) LEED pattern. The surface structure was also indirectly examined by SFG using CO as probe molecule. Only on clean smooth surfaces CO produces a perfect (2×2)-3CO structure that exhibits a characteristic vibrational spectrum (with narrow peaks at 1898 and 2109 cm^{-1}). After similar cleaning treatments, STM inspection by Mitsui et al.[46,47] revealed a low density of steps/defects (<5%) and a concentration of (subsurface) impurities (O, C, S) below 1%.

Methanol (p.a.) was cleaned by freeze−thaw cycles, and CO (99.997%) was purified using a liquid nitrogen cold trap and a carbonyl absorber cartridge. No contaminants were detected by MS or gas chromatography. For UHV exposures, the pressure indicated by the ionization gauge was corrected by the gauge sensitivity factors for CH_3OH (1.9) and CO (1.0); for experiments at 0.1 mbar, a Baratron gauge was used.

Results

Methanol Decomposition at 5×10^{-7} mbar. Figure 1 displays SFG and C1s XPS spectra, acquired at 5×10^{-7} mbar of CH_3OH at 300 K in intervals of 30 and 60 min, respectively. Figure 1a shows the stretching region of the decomposition product CO, with all SFG spectra exhibiting a single peak at ~1930 cm^{-1}. On the basis of our previous SFG/TDS/LEED/XPS studies of (pure) CO adsorption[8,34,35] and on literature data (e.g., refs 48-51), this peak originates from hollow- or bridge-bonded CO at a (local) coverage of ~0.5 ML. No signals were detected in the C−H stretching region (2600−3200 cm^{-1}), pointing to the absence or to a very low concentration of CH_3OH, CH_xO, and/or CH_x species. The SFG spectra indicated an immediate build-up of ~0.5 ML of CO and did not change within 210 min. Since 0.5 ML is the CO saturation coverage at 300 K (at low pressure), higher CO coverages were not obtained.

TABLE 1: Coverage (Monolayers, ML) of Carbon-Containing Species (CH_x and CO) on Pd(111) as a Function of CH_3OH Pressure, Reaction Temperature, and Time, As Determined by XPS

	coverage (ML)					
conditions	30 min	90 min	150 min	210 min	270 min	species
10^{-6} mbar of CH_3OH,	0.03	0.15	0.19	0.21	0.26	CH_x
at 300 K	0.48	0.47	0.47	0.47	0.43	CO
10^{-6} mbar of CH_3OH,	0.17	0.33	0.48	0.62	0.74	CH_x
at 400 K	0.19	0.17	0.16	0.17	0.17	CO
0.1 mbar of CH_3OH,	1.0	0.97	1.0	0.93		CH_x
at 300 K	0.50	0.48	0.41	0.37		CO
0.1 mbar of CH_3OH,	1.5	1.4	1.5			CH_x
at 400 K	0.32	0.28	0.32			CO

Figure 1c shows the corresponding C1s XPS spectra acquired at 5×10^{-7} mbar of CH_3OH at 300 K, with all spectra exhibiting two overlapping peaks at 285.6 and 283.7 eV (for the clean surface, the amount of residual carbon was below the XPS sensitivity level; see ref 8). A peak decomposition analysis using the Doniach−Šanjic function[52] is apparently necessary to extract the relative concentration of the carbon-containing species. According to the Shirley method,[53] the secondary (inelastically scattered) electron background was assumed to be nonlinear for the C1s and Pd3d spectra. Results of fitting two components to the C1s spectra as well as the original data points are included in Figure 1c (C1s spectra were normalized to the Pd3d integral intensity). Figure 1d displays the extracted quantitative information, which is also summarized in Table 1.

The peak at 285.6 eV essentially remained constant and, according to its binding energy, may be assigned to a CH_xO ($x = 0-4$) species, i.e., possible candidates are methanol (CH_3OH), methoxy (CH_3O), and other dehydrogenation products (CH_2O, HCO), as well as CO. Quantitative analysis of the 285.6 eV peak indicated a coverage of ∼0.5 ML (Figure 1d; using well-known CO/Pd(111) structures as reference,[8] as described above). Since the same coverage was observed for CO by SFG, the peak at 285.6 eV is most likely (nearly exclusively) due to adsorbed CO, which is also supported by previous studies.[12−27] Above ∼150 K, dissociative chemisorption of methanol occurred, producing surface methoxy (CH_3O) groups, and around 250−300 K decomposition to adsorbed CO and hydrogen was observed. For instance, CH_3O-related features, which were identified by high-resolution electron energy loss spectroscopy (HREELS) after methanol adsorption on Pd(111) at low temperature (200−250 K), fully disappeared after heating the adsorbed layer to 300 K. If methanol was adsorbed directly at 300 K, only CO-related features were detected by HREELS.[15,18,21] However, due to the limited resolution of our photoelectron spectrometer, we cannot differentiate between hollow- and bridge-bonded CO. According to a previous high-resolution XPS study,[51] both species may be present at 300 K.

In contrast to the dehydrogenation product CO, the coverage of the second feature (283.7 eV) increased with time (Figure 1c,d). On the basis of typical C1s binding energies of surface carbon atoms or hydrocarbon moieties on transition metals (282−285 eV),[54] we assign the growing C1s peak at 283.7 eV to adsorbed CH_x ($x = 0-3$) species. According to XPS, the amount of CH_x species is ca. 0.2 ML after 210 min (Table 1). This was apparently too low to induce significant changes in the CO−SFG spectrum during methanol decomposition (Figure 1a). However, the location of the CH_x species can be examined by comparing pre- and postreaction CO adsorption spectra (Figure 1b), which probe the availability of adsorption sites on Pd(111) [surface saturated with CO by cooling Pd(111) from 300 to 90 K in 3×10^{-6} mbar of CO].[34,35]

Before CH_3OH exposure, i.e., on the clean surface, a (2×2)-3CO saturation structure (0.75 ML) was observed, with CO bonded to fcc and hcp 3-fold hollow sites and on-top sites (Figure 1b; with peaks at 1898 and 2109 cm^{-1}, respectively). After methanol decomposition, i.e., after exposing Pd(111) for 210 min to 5×10^{-7} mbar of methanol at 300 K, a different saturation structure was observed, exhibiting hollow (∼1885 cm^{-1}), bridge (1938 cm^{-1}), and two on-top CO features (2091 and 2105 cm^{-1}) (Figure 1b). This together with the approximately 2-fold reduced intensity of hollow (and on-top) bonded CO reveals that part of the hollow sites are blocked by CH_x and that the CO layer is steered in a configuration that includes domains with 0.75 ML (hollow/on-top) and lower (∼0.65 ML; bridge/on-top) coverage. Similar spectra ("non-equilibrium structures") can also be observed on clean Pd(111), but only upon low-temperature ($T < 150$ K) CO exposure, when the CO mobility is not high enough to produce well-ordered (2×2) layers.[35,55,56] However, such structures were avoided in Figure 1b by cooling Pd(111) from 300 to 90 K in 3×10^{-6} mbar of CO. The observed change in CO adsorption is therefore due to site blocking by CH_x. Irreversible surface restructuring induced by CH_3OH or CO can also be excluded, since no peaks around 1990 cm^{-1} were observed in the postreaction spectra (Figure 1b), which would be characteristic for surface defects.[34,44]

The preferred binding of CH_x to hollow sites may also reveal its stoichiometry (i.e. the value of "x"). According to theoretical studies,[57,58] CH_x ($x = 0-3$) fragments tend to restore their tetravalency on the surface: adsorbed carbon atoms and CH species prefer hollow sites, CH_2 preferentially binds to bridge sites, and CH_3 sits on top of Pd atoms. Consequently, the partial blocking of hollow sites suggests the presence of carbon atoms and/or CH species. This is also supported by the absence of C−H signals in SFG and by XPS literature data: isolated carbon species occupying 3-fold hollow sites[57] were characterized by a C1s binding energy of 283.7 eV.[54] However, since this assignment cannot be unambiguously proven and small CH_x coverages may not be detected by SFG, carbonaceous species are still termed "CH_x" below.

Corresponding SFG/XPS experiments were also carried out at 400 K, as shown in Figure 2. The SFG spectra display only a weak and broad resonance around 1890−1860 cm^{-1}, characteristic of hollow-bonded CO at coverages of ≤0.3 ML (the small signal intensity presumably originates from the increased line width and the faster CH_x deposition).[34] A partial population of bridge sites cannot be excluded though.[51] The CO coverage was again constant with time (Figure 2d). In XPS, two overlapping peaks at 285.6 and 284.0 eV were observed (Figure 2c) and once more attributed to adsorbed CO and CH_x, respectively. As mentioned, hollow- and bridge-bonded CO species are not resolved in our XPS spectra. The steady-state CO coverage was ∼0.2 ML, in reasonable agreement with the estimation from SFG. The CH_x concentration increased continuously, reaching about 0.75 ML after 270 min (Figure 2d and Table 1). Postreaction CO−SFG at 90 K again indicated a partial

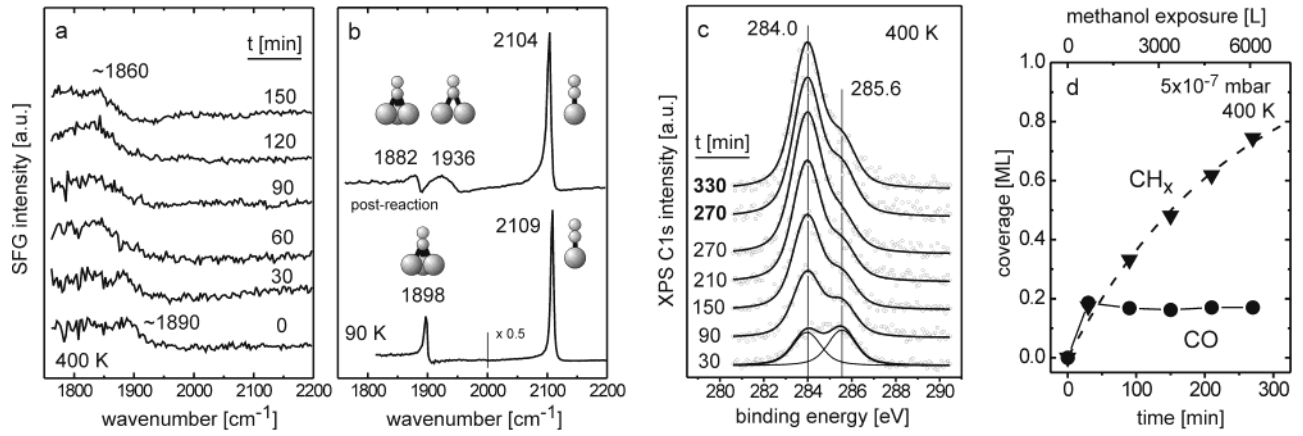

Figure 2. SFG (a) and XPS C1s core-level (c) spectra measured during exposure of Pd(111) to 5×10^{-7} mbar of methanol at 400 K. The upper two XPS spectra were measured after 270 and 330 min of methanol exposure without X-ray irradiation. The quantitative analysis of the XPS spectra is shown in panel d, and pre- and postreaction CO adsorption is compared in panel b. The dashed line in d is the calculated rate of CH_x formation obtained by assuming a simple kinetic model in which the CH_x formation rate is proportional to the number of vacant sites; see the text.

blocking of hollow (and on-top) sites by CH_x, suggesting the presence of carbon or CH species on the surface. One should also note that the C1s binding energy of CH_x at 400 K (284.0 eV) was 0.3 eV higher than at 300 K (283.7 eV). This may indicate that the structure of the carbonaceous residues at 400 K is different from that at 300 K (as discussed below).

We have also performed "blank" experiments, i.e., without X-ray irradiation, that show that methanolic C−O bond scission is not photoinduced. The two uppermost spectra in Figure 2c were measured after exposing Pd(111) for 270 and 330 min to 5×10^{-7} mbar of methanol at 400 K, but *without* X-ray irradiation. Comparison of the 270 min spectra shows that the rate of CH_x production was the same with and without X-ray irradiation.

An interesting point to note is that the initial rate of CH_x deposition was high both at 300 and 400 K ($\sim 1.7 \times 10^{-3}$ ML/min at 300 K, $\sim 5.7 \times 10^{-3}$ ML/min at 400 K). It then dropped after 90 min at 300 K (from $\sim 1.7 \times 10^{-3}$ to $\sim 6.1 \times 10^{-4}$ ML/min) and after 30 min at 400 K (from $\sim 5.7 \times 10^{-3}$ to $\sim 2.3 \times 10^{-3}$ ML/min), when a CH_x coverage of about 0.2 ML was reached but then remained fairly constant. Recently, a similar kinetic effect was observed for methanol decomposition on Pd nanoparticles.[28] It was attributed to fast C−O bond scission on particle edges, which are then preferentially blocked by CH_x, while slow C−O bond scission was attributed to the (111) facets of the nanoparticles. On Pd(111), this behavior does not necessarily indicate a defect-induced mechanism of methanolic C−O bond scission. We suggest that the C−O bond scission is initially fast because the CH_x coverage is low (while a given CO coverage is instantaneously built-up and then rather stays constant). Indeed, the decomposition of adsorbed CH_3OH, methoxy or other CH_xO species will require one or more vacant metal sites where products/fragments of the dissociation reaction can reside. With increasing CH_x coverage the vacant sites are more and more occupied, leading to a site-blocking mechanism that decreases the rate of methanol decomposition. The dashed lines in Figures 1d and 2d are calculated rates (amounts) of CH_x formation obtained by assuming a simple first-order kinetic model where the CH_x formation rate is proportional to the number of vacant surface sites ($r(CH_x)_t = d[CH_x]/dt = k[*]_t[CH_3OH]^0$). Assuming zero-order dependence in methanol (since the overall conversion is nearly zero) and $[*]_t = [*]_{t=0} - [CH_x]_t$, it follows that $[CH_x]_t = [*]_{t=0}(1 - e^{-kt})$, with k being the rate constant and $[*]_{t=0}$ the initial concentration of vacant surface sites (due to the immediate build-up of CO, this value is smaller than 1 ML). The lines fit the measured data points reasonably well without including a defect-induced mechanism of C−O bond scission on Pd(111) under our conditions. Of course, surface defects may still exhibit the highest bond-breaking activity, but they will also be rapidly poisoned by carbon. On the basis of these observations, we state that at elevated pressure methanolic C−O bond scission readily occurs, even on Pd(111).

Methanol Decomposition at 0.1−15 mbar. SFG and XPS spectra of methanol decomposition at 0.1 mbar and 300 K are collected in Figure 3. The SFG spectra (Figure 3a) show two nearly constant peaks, one dominating peak at 1929−1920 cm^{-1}, characteristic of ~0.5 ML of bridge- or hollow-bonded CO, and a second weak and broad feature at ~2075−2065 cm^{-1}, pointing to on-top CO. The appearance of the broad on-top signal when the bridge signal is found at ~1925 cm^{-1} is unusual. For low-temperature (UHV) CO spectra (cf. Figure 1 of refs 34 and 35), a peak at 1900−1920 cm^{-1} (CO coverage ≤ 0.5 ML) is *not* accompanied by an on-top signal, and on-top typically appears only after the CO frequency is shifted to ~1940 cm^{-1} or higher (CO coverage ≥ 0.6 ML). Although this cannot be fully explained, the large CH_x coverage may be partly responsible for the broad on-top feature observed under these conditions. Also, the presence of adsorbed hydrogen cannot be ruled out, because very similar spectra were observed for CO/H_2 mixtures [the Pd−H stretch (~500 cm^{-1}) is outside the frequency range accessible by our SFG spectrometer; for details, see ref 35].

XPS revealed three peaks at 0.1 mbar, i.e., at 287.6, 285.6, and 283.8 eV (Figure 3c). The first peak is the gas-phase signal of CH_3OH, which typically appeared above 10^{-2} mbar, while the other peaks are again due to CO (285.6 eV) and CH_x (283.8 eV). The surface concentration of CH_x species was about 1 ML already after the first measurement (Figure 3d and Table 1). Even though the total CH_x signal hardly changed with time, the CO coverage slowly decreased (from 0.5 to 0.37 ML), pointing to a continuous poisoning of adsorption sites (Figure 3d and Table 1). Nevertheless, the high surface concentration of CO indicates that despite monolayer coverage of CH_x a large part of the Pd(111) surface seems to be still free from carbonaceous residues.

Removal of the CH_3OH gas phase (Figure 3c) did not change the C1s spectrum (apart from the CH_3OH gas-phase signal), indicating that there were no (significant) contributions from weakly bonded surface species. However, a shift of the CH_x

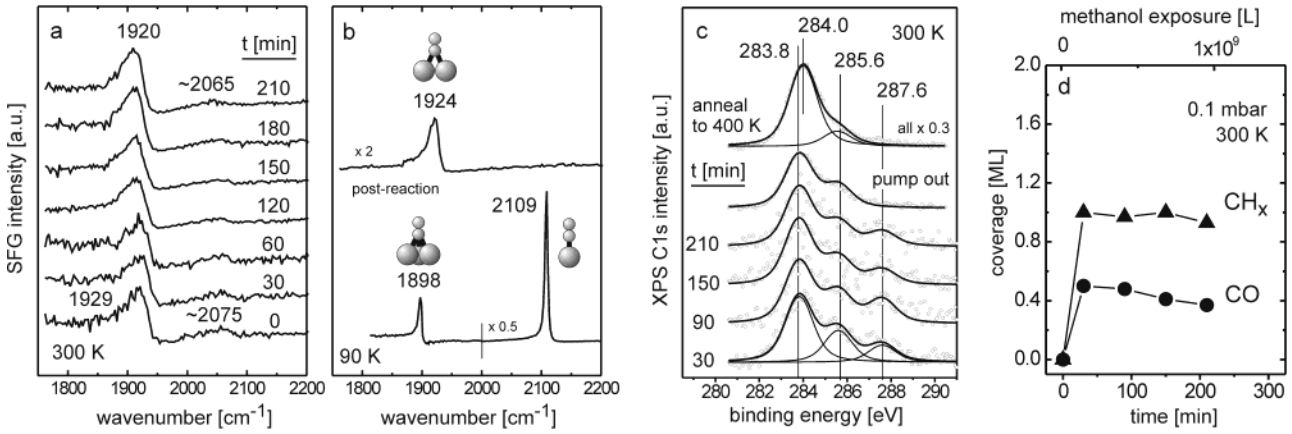

Figure 3. SFG (a) and XPS C1s core-level (c) spectra measured during exposure of Pd(111) to 0.1 mbar of methanol at 300 K. The quantitative analysis of the XPS spectra is shown in panel d, and pre- and postreaction CO adsorption is compared in panel b.

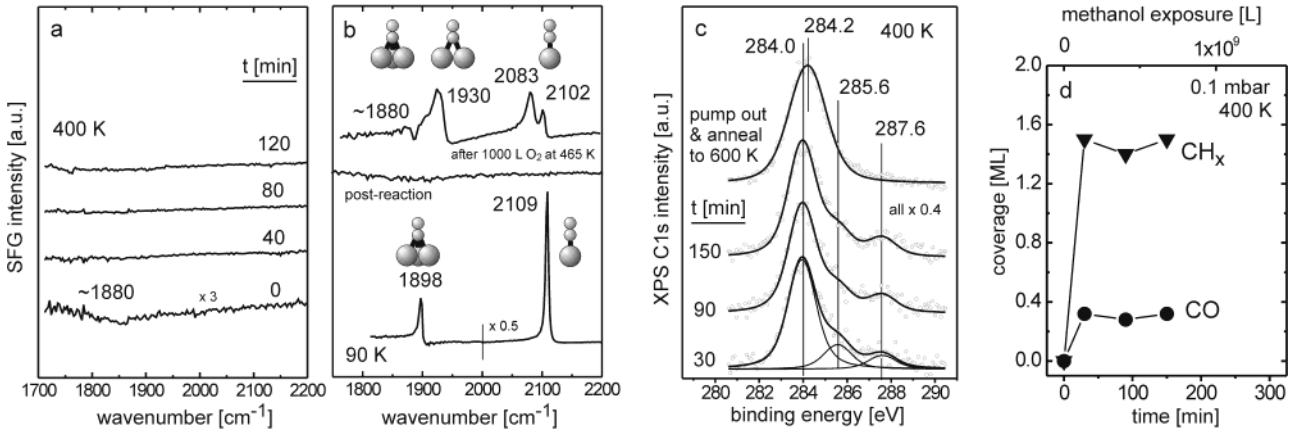

Figure 4. SFG (a) and XPS C1s core-level (c) spectra measured during exposure of Pd(111) to 0.1 mbar of methanol at 400 K. The quantitative analysis of the XPS spectra is shown in panel d, and pre- and postreaction CO adsorption is compared in panel b.

component to 284.0 eV and a reduction of the CO component due to partial CO desorption were observed after heating to 400 K in a vacuum.

While the SFG spectra in Figure 3a did not strongly reflect the increased amount of CH_x (as compared to Figure 1), postreaction SFG with CO as probe molecule in fact indicated a higher CH_x concentration (Figure 3b). CO was now no longer able to populate hollow or on-top sites. A single peak at 1924 cm^{-1}, rather typical of bridge-bonded CO, was observed after methanol decomposition. Hollow sites are most likely physically blocked by CH_x, which also influences the neighboring on-top sites, an effect that has also been observed for CO on carbon-covered Ni(100).[36]

At 400 K and 0.1 mbar of CH_3OH (Figure 4a), a very weak resonance was observed in the first SFG spectrum (~1880 cm^{-1}; CO coverage < 0.3 ML), while the subsequent spectra did not indicate resonances anymore. Postreaction CO−SFG suggested a fully carbon-covered Pd surface, since no CO adsorption occurred (Figure 4b). XPS spectra of 0.1 mbar of CH_3OH at 400 K detected ~1.5 ML of CH_x (284.0 eV) and ~0.3 ML of CO (285.6 eV), apart from the CH_3OH gas-phase signal at 287.6 eV (Figure 4c,d). This again suggests that part of the Pd(111) surface remains free from carbon. After removal of the gas phase and annealing to 600 K, XPS indicated that CO had desorbed while the CH_x species was apparently thermally stable (Figure 4c). However, a shift to 284.2 eV points to a structural change of the carbon overlayer.

The chemical stability of the CH_x species produced by CH_3OH decomposition at 300 or 400 K (~1−1.5 ML; Figures 3c and 4c) toward oxygen was also investigated. Upon exposing the carbon- and CO-poisoned Pd(111) surface to 10^{-2} mbar of oxygen at 300 K, no changes were detected by C1s XPS within 0.5 h, i.e., the two features of CH_x and adsorbed CO maintained their intensity. This suggests that the CH_x- and CO-covered surface provided no sites for dissociative oxygen adsorption. Otherwise, oxygen atoms should react with CO to give CO_2, which would desorb from the surface at 300 K. Alternatively, the reaction of CO and oxygen may be simply too slow at 300 K.[59] In contrast, all C1s features immediately disappeared at 400 K in 10^{-2} mbar of oxygen. CO desorption around 400 K produced vacant sites for dissociative oxygen adsorption that reacted away CH_x. After treating the carbon-poisoned surface (Figure 4b) with 1000 L of O_2 at 465 K, CO−SFG at 90 K indicated a partial recovery of the initial adsorption properties (Figure 4b, uppermost trace).

CH_3OH decomposition was also carried out at 15 mbar of CH_3OH (with He as fill-up gas to 1 bar), using gas chromatography with thermal conductivity detection for product analysis. At 300−550 K, the CH_3OH GC signal remained constant for several hours, and no decomposition products (such as CO, CH_4, or H_2O) were detected. Apparently, carbonaceous deposits again rapidly poisoned the Pd surface. When 15 mbar of oxygen was added at 450 K, CH_x could again be easily removed and CH_3OH was immediately oxidized to CO_2 and H_2O.

CO Adsorption at 10^{-6}−0.1 mbar. For completeness we also want to mention that no carbon was observed upon exposure of 10^{-6}−0.1 mbar of CO at 300 and 400 K.[8] C1s core-level spectra exhibited a single peak at ~285.5 eV (molecular CO), while SFG revealed bridge and/or 3-fold hollow-bonded CO

and varying amounts of on-top CO (total coverage ca. 0.4−0.65 ML; for details, see ref 8). Carbon deposits (amorphous, graphitic, etc.) that typically appear at ∼284 eV were not detected, excluding CO as source of the CH_x species. Therefore, the carbonaceous deposits observed in Figures 1−4 must originate from scission of the methanolic C−O bond within CH_xO and not from the dissociation of the decomposition product CO.

Discussion

The interaction of methanol with Pd(100),[13,14] Pd(110),[15,16] and Pd(111)[17−27] single-crystal surfaces was studied extensively under UHV conditions. All investigations agree that methanol adsorbs intact at low temperature, either as isolated methanol species or as multilayers of hydrogen-bonded methanol molecules.[12,13] Above ∼150 K, dissociative chemisorption of methanol occurs, producing surface methoxy (CH_3O) groups, and at 200−300 K decomposition to adsorbed CO and hydrogen was observed. CO desorbs over a wide temperature range with a maximum at ∼490 K, whereas associative hydrogen desorption takes place at ∼310 K.[13,14,17,19,20,35,60]

Our SFG/XPS results obtained at 5×10^{-7} mbar of CH_3OH are in line with the literature data. SFG spectra, showing a single peak typical of hollow-/bridge-bonded CO, indicate that only CO is produced during methanol interaction with Pd(111) at $T \geq 300$ K (Figures 1a and 2a), while no or only small amounts of intermediate decomposition products (CH_xO) are present. Taking into account the strong dependence of the CO stretching frequency on coverage,[8,34,44] approximately half-monolayer coverage of CO can be deduced from the resonance at ∼1925 cm^{-1} at 300 K. This is in quantitative agreement with the coverage detected by XPS for the C1s feature at 285.6 eV, leading to the conclusion that adsorbed CO *alone* contributed to the C1s signal. These and previous literature data indicate that dehydrogenation to CO and hydrogen is the main route of methanol decomposition in UHV.

The possibility of C−O bond scission during methanol decomposition on Pd(111) caused more debates in the literature. Scission of the methanolic C−O bond on Pd(111) was first reported by Winograd and co-workers,[23,24] applying XPS, secondary ion mass spectroscopy (SIMS), and TPD. On the basis of the coverage and temperature dependence of C−O bond scission, these authors suggested a bimolecular mechanism in which two neighboring adsorbed methanol molecules produce a methoxy and a methyl group on the surface (and water). Adsorption of methanol at 110 K and subsequent heating to 175 K in UHV lead to a carbon deposition of ∼0.04 ML. Guo et al.[19] also examined the possibility of methanolic C−O bond cleavage on Pd(111) at various adsorption temperatures from 87 to 265 K by isotopic mixing studies. Contrary to the results of Winograd et al.,[23,24] no indications of C−O bond scission were detected by TPD experiments with a sensitivity limit of 0.01 ML. Using XPS and SIMS, Rebholz et al.[25−27] found that the dominant route is the complete dehydrogenation to CO, but a small amount of adsorbed CH_3 species (∼0.05 ML) was also detected. To explain the experimental disagreement, it has been suggested that methanolic C−O bond scission requires surface defects or near monolayer CH_3OH coverage.

Our SFG/XPS data (Figures 1 and 2) show unambiguously that the scission of the methanolic C−O bond can proceed even on Pd(111). This conclusion is based on the accumulation of the C1s signal at ∼284 eV and a continuous lowering of the CO coverage due to a continuous blocking of hollow sites by adsorbed CH_x. The rate of CH_x formation increases with temperature and pressure, and CH_x coverages as large as ∼1−1.5 ML can be reached at 0.1 mbar of CH_3OH (Figures 3 and 4).

Another question discussed in the literature is the nature of the carbonaceous residue. In their studies of methanol decomposition, Rebholz et al.[25−27] reported that methyl fragments (CH_3) formed at ∼200 K were stable up to 500 K. Similar to this, Chen et al.[24] found that CH_3 was stable up to 400 K; above 400 K stepwise dehydrogenation to CH_2 (methylene), CH (methylidyne), and C occurred. In contrast, Solymosi et al.[61,62] reported that CH_3 species produced by CH_3I decomposition on Pd(100) below 250 K fully dehydrogenated to C already above 300 K, with no spectroscopic evidence for CH_2 and CH species.[63,64] Coadsorbed CO may enhance the thermal stability of methyl fragments, but only by 60−80 K as compared to clean palladium.[62,65]

Combining SFG and XPS allowed us to obtain further information on the CH_x species that rather supports the picture of strongly dehydrogenated or even carbon species. SFG did not show any C−H stretch signals from CH_x ($x = 1-3$) fragments (2700−3200 cm^{-1}) and also the XPS C1s binding energy values rather correspond to the formation of carbon atoms. Indeed, isolated carbon atoms exhibit a lower C1s binding energy (283.7−283.8 eV)[54,66] than adsorbed hydrocarbons (>284.2 eV). Furthermore, XPS as well as postreaction CO−SFG pointed to the coexistence of relatively large amounts of CO and CH_x (e.g. ∼0.5 ML of CO and ∼1 ML of CH_x in Figure 3). This suggests that carbon either partly moves to subsurface regions or produces three-dimensional carbon clusters on the palladium surface.

Carbon dissolution seems possible, because the migration of atomic carbon from a surface hollow site to an octahedral subsurface site is almost isoenergetic, as shown by the density functional study of Yudanov et al.[67] Because this dissolved carbon resides within a few layers below the surface (and is still accessible to XPS), this picture is not necessarily in contrast to the commonly accepted temperature range of carbon dissolution in the Pd bulk (around 700 K), when carbon signals disappear in XPS.[24,68,69] Dissolved carbon may also change the CO adsorption energy[67,68] and may be an alternative explanation for the absence of on-top CO in Figure 3b (beside a site blocking effect by neighboring hollow-bonded surface carbon).

The observed shift of the CH_x C1s XPS signals to higher binding energy upon heating the Pd(111) surface after methanol decomposition (Figures 3c and 4c) may also point to the possible formation of carbon islands or clusters. An increase in the C1s binding energy was reported when the structure of carbonaceous residues changed from a row of isolated atoms (283.8 eV), to carbon chains (284.2 eV), to graphene (284.4 eV), and to graphitic islands (284.6 eV).[54]

Unfortunately, neither XPS nor SFG allows an unambiguous discrimination between the two possibilities. Despite this, it is clear that only highly dehydrogenated carbon species can participate in carbon dissolution or agglomeration processes. Taking into account all results, we suggest that even at 300 K, dehydrogenation of CH_x to surface carbon and hydrogen occurs immediately after CH_x formation by methanolic C−O bond scission.

The occurrence of methanolic C−O bond scission and the absence of CO dissociation can be rationalized along the following lines.[31,70] While CO binds to Pd via the carbon atom and with the C−O bond perpendicular to the surface,[71,72] methoxy CH_3O binds to the surface via the oxygen atom.[12,30,73] Apart from the influence of the additional hydrogen atoms in

the molecule, in the subsequent dehydrogenation products (CH_2O, CHO) the oxygen *and* the carbon atom may both bind to the surface,[31,70,73] resulting in a C−O bond that is tilted with respect to the Pd substrate. A tilted C−O bond seems to facilitate C−O bond scission due too a better overlap between the metal valence electron density and the CH_xO orbitals (which weakens the C−O bond).[70] In contrast, C−O scission within the "upright" product molecule CO is unfavorable, as recently confirmed by our combined high-pressure SFG/XPS studies.[8] A similar relationship between the adsorption geometry and C−O bond activation may also hold for higher alcohols.[31]

Conclusions

SFG, XPS, and GC studies of CH_3OH decomposition on Pd(111) clearly show that at elevated pressure (5×10^{-7}−15 mbar) CH_3OH decomposition to CO and H_2 does only occur to a small extent. There is a rapid self-poisoning by adsorbed CO and CH_x at 300 K, while at 400 K the fast formation of CH_x layers (around 1 ML) prevents a significant conversion. This indicates that Pd(111) is in fact able to break the methanolic C−O bond, but its observation may require a sufficient CH_3OH impingement rate above ∼250 K. To produce CO and H_2 from CH_3OH on Pd catalysts, the CH_x formation must be suppressed or CH_x must be selectively removed/oxidized without total oxidation of methanol.

Acknowledgment. M.M. acknowledges financial support from DFG (project SPP 1091). V.V.K. is grateful for fellowships granted by DAAD and the Max Planck Society.

References and Notes

(1) Wickham, D. T.; Logsdon, B. W.; Cowley, S. W.; Butler, C. D. *J. Catal.* **1991**, *128*, 198.
(2) Matsumura, Y.; Okumura, M.; Usami, Y.; Kagawa, K.; Yamashita, H.; Anpo, M.; Haruta, M. *Catal. Lett.* **1997**, *44*, 189.
(3) Usami, Y.; Kagawa, K.; Kawazoe, M.; Matsumura, Y.; Sakurai, H.; Haruta, M. *Appl. Catal. A: Gen.* **1998**, *171*, 123.
(4) Shiozaki, R.; Hayakawa, T.; Liu, Y. Y.; Ishii, T.; Kumagai, M.; Hamakawa, S.; Suzuki, K.; Itoh, T.; Shishido, T.; Takehira, K. *Catal. Lett.* **1999**, *58*, 131.
(5) Matolín, V.; Stará, I.; Tsud, N.; Johánek, V. *Prog. Surf. Sci.* **2001**, *67*, 167.
(6) Henry, C. R.; Chapon, C.; Goyhenex, C.; Monot, R. *Surf. Sci.* **1992**, *272*, 283.
(7) Cordatos, H.; Bunluesin, T.; Gorte, R. J. *Surf. Sci.* **1995**, *323*, 219.
(8) Kaichev, V. V.; Prosvirin, I. P.; Bukhtiyarov, V. I.; Unterhalt, H.; Rupprechter, G.; Freund, H.-J. *J. Phys. Chem. B* **2003**, *107*, 3522.
(9) Poutsma, M. L.; Elek, L. F.; Ibarbia, P. A.; Risch, A. P.; Rabo, J. A. *J. Catal.* **1978**, *52*, 157.
(10) Fajula, F.; Anthony, R. G.; Lunsford, J. H. *J. Catal.* **1982**, *73*, 237.
(11) Kelly, K. P.; Tatsumi, T.; Uematsu, T.; Driscoll, D. J.; Lunsford, J. H. *J. Catal.* **1986**, *101*, 396.
(12) Lüth, H.; Rubloff, G. W.; Grobmann, W. D. *Surf. Sci.* **1977**, *63*, 325.
(13) Christmann, K.; Demuth, J. E. *J. Chem. Phys.* **1982**, *76*, 6308.
(14) Solymosi, F.; Berkó, A.; Tóth, Z. *Surf. Sci.* **1993**, *285*, 197.
(15) Bhattacharya, A. K.; Chesters, M. A.; Pemble, M. E.; Sheppard, N. *Surf. Sci.* **1988**, *206*, L845.
(16) Hartmann, N.; Esch, F.; Imbihl, R. *Surf. Sci.* **1993**, *297*, 175.
(17) Kok, G. A.; Noordermeer, A.; Nieuwenhuys, B. E. *Surf. Sci.* **1983**, *135*, 65.
(18) Gates, J. A.; Kesmodel, L. L. *J. Catal.* **1983**, *83*, 437.
(19) Guo, X.; Hanley, L.; Yates, J. J. T. *J. Am. Chem. Soc.* **1989**, *111*, 3155.
(20) Davis, J. L.; Barteau, M. A. *Surf. Sci.* **1987**, *187*, 387.
(21) Davis, J. L.; Barteau, M. A. *Surf. Sci.* **1990**, *235*, 235.
(22) Francis, S. M.; Corneille, J.; Goodman, D. W.; Bowker, M. *Surf. Sci.* **1996**, *364*, 30.
(23) Levis, R. J.; Zhicheng, J.; Winograd, N. *J. Am. Chem. Soc.* **1989**, *111*, 4605.
(24) Chen, J.-J.; Jiang, Z.-C.; Zhou, Y.; Chakraborty, B. R.; Winograd, N. *Surf. Sci.* **1995**, *328*, 248.
(25) Rebholz, M.; Matolin, V.; Prins, R.; Kruse, N. *Surf. Sci.* **1991**, *251*−*252*, 1117.
(26) Kruse, N.; Rebholz, M.; Matolin, V.; Chuah, G. K.; Block, J. H. *Surf. Sci.* **1990**, *238*, L457.
(27) Rebholz, M.; Kruse, N. *J. Chem. Phys.* **1991**, *95*, 7745.
(28) Schauermann, S.; Hoffmann, J.; Johánek, V.; Hartmann, J.; Libuda, J.; Freund, H.-J. *Catal. Lett.* **2002**, *84*, 209.
(29) Schennach, R.; Eichler, A.; Rendulic, K. D. *J. Phys. Chem. B* **2003**, *107*, 2552.
(30) Zhang, C. J.; Hu, P. *J. Chem. Phys.* **2001**, *115*, 7182.
(31) Mavrikakis, M.; Barteau, M. *J. Mol. Catal. A* **1998**, *131*, 135.
(32) Levis, R. J.; Zhicheng, J.; Winograd, N. *J. Am. Chem. Soc.* **1988**, *110*, 4431.
(33) Freund, H.-J.; Bäumer, M.; Libuda, J.; Risse, T.; Rupprechter, G.; Shaikhutdinov, S. *J. Catal.* **2003**, *216*, 223.
(34) Rupprechter, G.; Unterhalt, H.; Morkel, M.; Galletto, P.; Hu, L.; Freund, H.-J. *Surf. Sci.* **2002**, *502*−*503*, 109.
(35) Morkel, M.; Rupprechter, G.; Freund, H.-J. *J. Chem. Phys.* **2003**, *119*, 10853.
(36) Rupprechter, G.; Dellwig, T.; Unterhalt, H.; Freund, H.-J. *Top. Catal.* **2001**, *15*, 19.
(37) Rupprechter, G. *Phys. Chem. Chem. Phys.* **2001**, *3*, 4621.
(38) Shen, Y. R. *Surf. Sci.* **1994**, *299*/*300*, 551.
(39) Somorjai, G. A.; Rupprechter, G. *J. Phys. Chem. B* **1999**, *103*, 1623.
(40) McCrea, K. R.; Somorjai, G. A. *Adv. Catal.* **2000**, *45*, 385.
(41) Chen, Z.; Shen, Y.-R.; Somorjai, G. A. *Annu. Rev. Phys. Chem.* **2002**, *53*, 437.
(42) Härle, H.; Mendel, K.; Metka, U.; Volpp, H. R.; Willms, L.; Wolfrum, J. *Chem. Phys. Lett.* **1997**, *279*, 275.
(43) Bandara, A.; Dobashi, S.; Kubota, J.; Onda, K.; Wada, A.; Domen, K.; Hirose, C.; Kano, S. *Surf. Sci.* **1997**, *387*, 312.
(44) Unterhalt, H.; Rupprechter, G.; Freund, H.-J. *J. Phys. Chem. B.* **2002**, *106*, 356.
(45) Kaichev, V. V.; Sorokin, A. M.; Timoshin, A. I.; Vovk, E. I. *Instrum. Exp. Techniques* **2002**, *45*, 50.
(46) Mitsui, T.; Rose, M. K.; Fomin, E.; Ogletree, D. F.; Salmeron, M. *Surf. Sci.* **2002**, *511*, 259.
(47) Rose, M. K.; Borg, A.; Mitsui, T.; Ogletree, D. F.; Salmeron, M. *J. Chem. Phys.* **2001**, *115*, 10927.
(48) Tüshaus, M.; Berndt, W.; Conrad, H.; Bradshaw, A. M.; Persson, B. *Appl. Phys. A* **1990**, *51*, 91.
(49) Hoffmann, F. M. *Surf. Sci. Rep.* **1983**, *3*, 103.
(50) Rose, M. K.; Mitsui, T.; Dunphy, J.; Borg, A.; Ogletree, D. F.; Salmeron, M.; Sautet, P. *Surf. Sci.* **2002**, *512*, 48.
(51) Surnev, S.; Sock, M.; Ramsey, M. G.; Netzer, F. P.; M.Wiklund; Borg, M.; Andersen, J. N. *Surf. Sci.* **2000**, *470*, 171.
(52) Doniach, S.; Šanjic, M. *J. Phys. C.* **1970**, *3*, 285.
(53) Shirley, D. A. *Phys. Rev. B* **1972**, *5*, 4709.
(54) Rodriguez, N. M.; Anderson, P. E.; Wootsch, A.; Wild, U.; Schlögl, R.; Paal, Z. *J. Catal.* **2001**, *197*, 365.
(55) Morkel, M.; Unterhalt, H.; Salmeron, M.; Rupprechter, G.; Freund, H.-J. *Surf. Sci.* **2003**, *532*−*535*, 103.
(56) Bourguignon, B.; Carrez, S.; Dragnea, B.; Dubost, H. *Surf. Sci.* **1998**, *418*, 171.
(57) Paul, J.-F.; Sautet, P. *J. Phys. Chem. B* **1998**, *102*, 1578.
(58) Zhang, C. J.; Hu, P. *J. Chem. Phys.* **2002**, *116*, 322.
(59) Libuda, J.; Freund, H.-J. *J. Phys. Chem. B* **2002**, *106*, 4901.
(60) Rupprechter, G.; Morkel, M.; Freund, H.-J.; Hirschl, R. *Surf. Sci.* **2004**, *554*, 43.
(61) Solymosi, F.; Révész, K. *J. Am. Chem. Soc.* **1991**, *113*, 9145.
(62) Solymosi, F. *Catal. Today* **1996**, *28*, 193.
(63) Solymosi, F.; Kovacs, I.; Révész, K. *Catal. Lett.* **1994**, *27*, 53.
(64) Solymosi, F.; Erdöhelyi, A.; Cserényi, J.; Felvégi, A. *J. Catal.* **1994**, *147*, 272.
(65) Chen, J.-J.; Winograd, N. *Surf. Sci.* **1994**, *314*, 188.
(66) Sock, M.; Eichler, A.; Surnev, S.; Andersen, J. N.; Klötzer, B.; Hayek, K.; Ramsey, M. G.; P.Netzer, F. *Surf. Sci.* **2003**, *545*, 122.
(67) Yudanov, I. V.; Neyman, K. M.; Rösch, N. *Phys. Chem. Chem. Phys.* **2004**, *6*, 116.
(68) Ratajczykowa, I. *J. Vac. Sci. Technol. A* **1983**, *1*, 1512.
(69) Ratajczykowa, I. *Surf. Sci.* **1985**, *152*/*153*, 627.
(70) Broden, G.; Rhodin, T. N.; Bruckner, C. F.; Benbow, R.; Hurych, Z. *Surf. Sci.* **1976**, *59*, 593.
(71) Plummer, E. W.; Eberhardt, W. *Adv. Chem. Phys.* **1982**, *49*, 533.
(72) Galletto, P.; Unterhalt, H.; Rupprechter, G. *Chem. Phys. Lett.* **2003**, *367*, 785.
(73) Desai, S. K.; Neurock, M.; Kourtakis, K. *J. Phys. Chem. B* **2002**, *106*, 2559.